Development of Extreme-Ultraviolet Light Source by Laser-Produced Plasma

Hiroaki NISHIMURA,[1] Shinsuke FUJIOKA,[1] Masashi SHIMOMURA, [1] Hirokazu SAKAGUCHI,[1]

Yuki NAKAI,[1] Tatsuya AOTA,[1] Takeshi KAI,[1] Katsunobu NISHIHARA,[1] Noriaki MIYANAGA,[1]

Yasukazu IZAWA,[1] Kunioki MIMA,[1] Atsushi SUNAHARA,[2] Yoshinori SHIMADA,[2]

and Shin-ichi NAMBA[3]

[1]*Institute of Laser Engineering, Osaka University, 2-6 Yamada-oka, SUita, Osaka 565-0871*

[2] *Institute for Laser Technology, 2-6 Yamada-oka, Suita, Osaka 565-0871*

[3]*Graduate School of Engineering, Hiroshima University, 1-4-1 Kagamiyama, Higashi-hiroshima, 7398527*

(Received January 25, 2008)

Extreme ultraviolet (EUV) radiation from laser-produced plasma has been studied for mass-production of the next generation semiconductor devices with EUV lithography. A full set of experimental databases are provided for a wide range of parameters of lasers and targets. These data are utilized directly as a technical guide-line for EUV source system design in the industry as well as used to benchmark the radiation hydrodynamic code, including equation-of-state solvers and advanced atomic kinetic models, dedicated for EUV plasma predictions. Present status of the LPP EUV source studies is presented.

Key Words: Laser produced plasma, Extreme Ultraviolet (EUV), Tin opacity

1. Introduction

EUV lithography (EUVL) has been chosen as one of key technologies to extend further integration of electric circuit manufacturing along the technical path, commonly referred to as the roadmap of the semiconductor industry. In order to print node sizes less than 32 nm, EUVL systems will require extensive technical transfer between industry and research institutes. In Japan, the EUVL Association (EUVA) was established in June 2002 under the auspices of the Ministry of Economy, Trade and Industry (METI) to accelerate the development of EUV lithography systems. In the fiscal year 2003, following the start of a new leading project for development of an EUV light source for advanced lithography under auspices of MEXT, the Institute of Laser Engineering, Osaka University has started intensive research on the laser-produced plasma (LPP) source[1-3].

2. Lithography system with LPP EUV source

The principle of the LPP EUVL system is shown in Fig, 1. The source plasma is generated with laser pulses synchronized at a high repetition-rate with successively supplied targets of small mass. EUV light from the plasma is collected with a multilayer-coated EUV mirror to transfer the light to the illumination system via the intermediate focus (IF). Circuit-patterns recorded on a reflective reticle are finally imaged on an EUV resist layer coated on the silicon wafer. In this system, ten EUV mirrors are used from the source plasma to the wafer so that overall transfer efficiency of EUV light from the source to the wafer becomes less than 1% since the highest reflectivity is 65% at 13.5 nm for a Mo/Si mirror. Specifications of EUV source are definitely fixed through

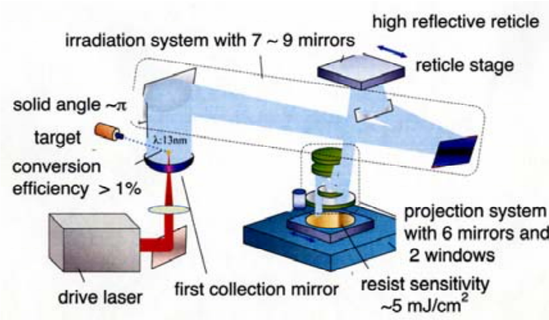

Fig.1 EUV light from the source plasma is collected by the first mirror, and transferred to the intermediate focus, at which the source power is defined.

discussions among industries[4]. These are listed in Table 1. Since the transfer efficiency from the first mirror to the IF is around 30% at highest, over 300 W EUV source power is required at plasma.

2.1 Prediction of plasma parameters

Among several candidates, Sn, Xe, and Li are considered to be the most promising materials due to the matching of their plasma spectra with reflection by Mo/Si multilayer mirror. Assume an etendue (defined by the product of the source area size and the light extraction solid angle) of 1 mm^2sr and an extraction solid angle of π; the area corresponds to that of a laser spot of 600 μm in diameter. It is required to extract EUV energy E_{EUV} of 30 to 40 mJ per pulse for 10 kHz repetition rate. Take an EUV pulse duration t_{EUV} of 1 to 10 ns; the EUV flux

Table 1. Specifications of EUV light source

wavelength	13.5 nm @2%BW
EUV power	> 180 W (@IF)
repetition rate	7-10 kHz or more
etendue	1-3.3 $mm^2 sr$
stability	+/- 0.3% 3σ over 50 pulses
source cleanliness	>30,000 hours at IF
spectral purity	
130-400 nm	<1% of EUV at wafer
> 400 nm	< 10-100% at wafer

*IF : intermediate focus, a point transferring EUV light to the illumination system.

I_{EUV} will be 10^9 to 10^{10} W/cm^2. If the conversion efficiency (CE) from laser to 13.5 nm EUV light in a 2% bandwidth (BW) is 1%, then the laser irradiance I_{LASER} will be $10^{11\text{-}12}$ W/cm^2. This flux is high enough to attain the plasma temperature of 60-70 eV.

The optimum ion density can be estimated from EUV photon flux Y_{EUV} (the number of photons emitted per unit area and unit time). Namely, Y_{EUV} is equal to $I_{EUV}/h\nu = 7\times10^{25}\text{-}7\times10^{26}$ photons/scm^2. This must balance with the value $(n_{EUV} \cdot l_{EUV})_{OD=1} \cdot A$, where n_{EUV} is the density of ions effectively contributing to EUV emission (define the efficiency as f), l_{EUV} is EUV plasma depth. Their product must be unity represented as optical density of 1, and A is Einstein A-coefficient. Since A^{-1} becomes around several 10 ps, the density-depth product $n_{EUV} l_{EUV}$ will be $10^{15\text{-}16}$ cm^{-2}. For f=0.1 and l_{EUV}=100 μm, the optimum ion density n_i will be around $10^{18\text{-}19}$ cm^{-3}.

Since laser intensity is at most $10^{11\text{-}12}$ W/cm^2 to generate EUV plasmas, the dominant absorption mechanism is classical. The ideal condition is that the absorption region corresponds to the EUV dominant region. l_{EUV} is simply given by the product of plasma sound velocity and laser pulse duration. In this way, one can obtain the optimum region as shown in Fig. 2 assuming that the product of l_{EUV} and the absorption coefficient is 1 to 2. From this picture, the optimum laser wavelength will be 2-3 mm although there are no laser candidates available for practical use. If laser wavelength is shorter than 1 mm, the shorter pulse duration is preferable. For long wavelength laser such as CO_2 laser, energy is deposited in a lower density region than that of the EUV dominant region, then the absorbed energy is transported mostly by thermal electrons. For shorter wavelength laser, such as an excimer laser, the energy is deposited in a higher density region, then EUV radiation generated there must pass through the EUV dominant region. This makes the EUV conversion efficiency (CE) lower due to the self-absorption (i.e., opacity effect) in the EUV dominant region.

2.2 A power balance model

In order to provide optimum plasma parameters, the radiation hydrodynamic code STAR[5] was developed. In parallel, a simple theoretical analysis has been made[6]. In the case of Sn plasma, EUV emission near 13-14 nm is arising from Δn=0 atomic transitions (n is the principal quantum number). Figure 3 shows typical density and temperature profiles of laser-produced Sn plasma. Also shown are

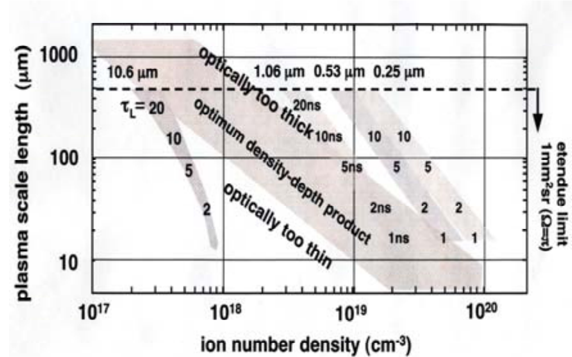

Fig. 2 Optimum plasma conditions predicted by a simple model. For shorter wavelength lasers, due to higher critical densities, shorter scale length is preferable for efficient EUV generation, and so.

emissivity profiles for the optically thin case and for the practical plasma case. Note that large difference is seen between them, particularly at higher density region due to the opacity effect.

A power balance model was made to deal with the loss fluxes due to ionization, plasma expansion, and radiation in EUV plasma. Physical parameters for the model calculation were derived from advanced atomic models such as HULLAC[7]. As is discussed below the model predictions were confirmed with simulations done with STAR. CEs at 13.5 nm within 2% bandwidth have been provided theoretically as a function of ion densities and electron temperatures for variety of laser conditions for Sn, Xe, and Li. The results are shown in Fig. 4.

3. Laser Plasma Experiments

3.1 Spherical plasma measurement

In previous EUV plasma experiments, a Joule-class, single laser beam was used. Therefore experimental results might be substantially influenced by energy flow along the target surface via plasma expansion and/or thermal conduction (so-called 2-D effect). In order to eliminate the problem for

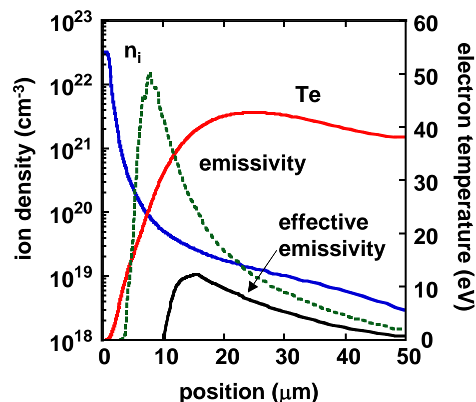

Fig. 3 Density, temperature, emissivities for the optically thin and practical cases are produced for Sn plasma with SATR[5].

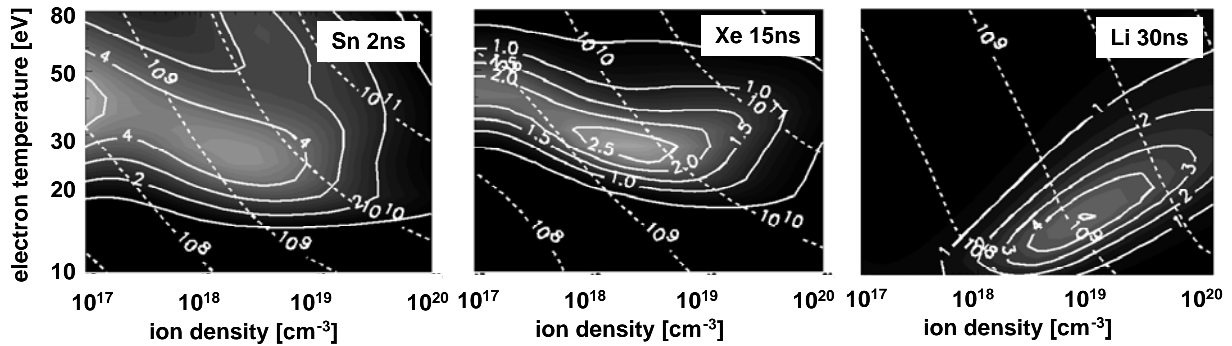

Fig. 4 EUV conversion efficiencies at 13.5 nm in a 2% BW are predicted with a simple power balance model as a function of ion density and electron temperature. The numbers on the solid circular lines represent the conversion efficiency in % and the dotted lines absorbed laser intensities needed to create plasma densities and temperatures in these maps.

comparison with theoretical interpretations, spherical targets were irradiated uniformly with GEKKO XII, a multiple-laser dedicated to laser fusion research[8]. Spherical plastic targets coated with a 1-μm-thick Sn layer, thick enough to generate EUV light, were used in the experiment. Figure 5 shows the CE dependence as a function of laser intensity. The CEs obtained with the two instruments agree quite well, showing the validity of mutual calibration processes. The highest CE of 3% was attained at an intensity of 0.5-1x1011 W/cm^2.

The CE dependence on the laser intensity was analyzed using the power balance model above. The result is also shown in Fig. 5 with a solid curve. A good agreement between the experiment and the prediction is obtained. Comparing the results of this study with Spitzer's investigation[9], we infer that even with a large laser spot size, the 2-D effect is not completely excluded, and thus a higher irradiance was needed. These results conclusively show that the formation of spherical plasma enables us to provide a good benchmark for theoretical models included in simulation codes.

3.2 Density profile measurement

Electron density profile of laser-produced Sn plasma was investigated using two interferometers to cover a wide range of density profiles[10]. Density profiles along the line of laser incidence extracted are plotted in Fig.6. Computer simulations were made using STAR code for 1-D and 2-D geometry (details are described below). A good agreement is obtained for the 2-D case. Discrepancy in 1-D simulation arises from the multi-dimension plasma expansion in experiment.

The EUV emission profile at the peak of laser pulse[11] is plotted in Fig.6 with dots. It is found that most of the EUV light comes from well under-dense plasma region with electron densities from 1×10^{19} cm^{-3} to 1×10^{20} cm^{-3}. The heavy re-absorption induced by the outer layer of plasma will reduce CE significantly. EUV emission near 13.5 nm can be attributed to *4d-4f*, *4p-4d*, and *4d-5p* transitions in Sn plasma with optimum temperature around 30 eV.

3.3 CE dependence on laser wavelength and pulse duration

Dependence of EUV CE on laser wavelengths was studied using ω, 2ω and 4ω light of Nd:YAG laser[12] and CO_2 laser[13]. EUV spectra generated with 532 nm and 266 nm lasers showed spectral dips around 13.5 nm and these features are well replicated in computer simulations. This infers existence of opaque plasma surrounding the EUV emission region. The CO_2 laser produced plasma has shown even higher CE than those generated with YAG ω light so that EUV source developers have chosen this laser as the most practical driver for EUV source generation.

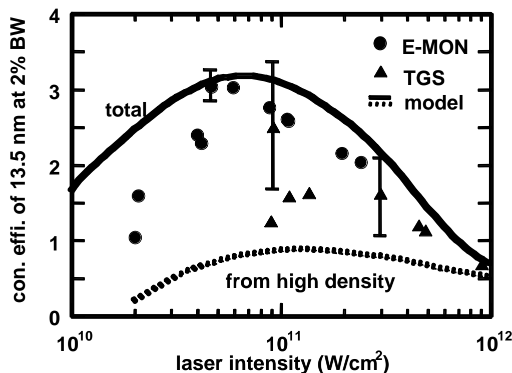

Fig. 5 Dependence of CE on laser intensity. The maximum CE of 3% was archived at the laser intensity of 0.5×10^{11} W/cm^2.[8]

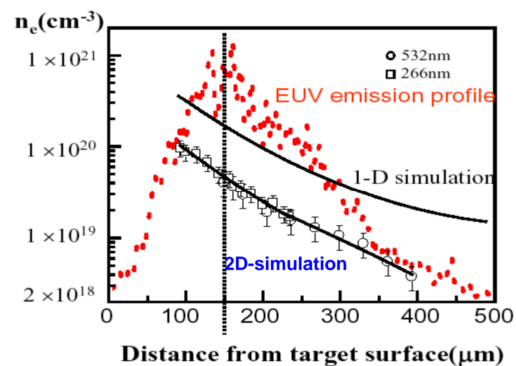

Fig 6. Electron density profiles from the 532 nm (circle), 266 nm (square) interferometers, 1-D and 2-D radiation hydrodynamic simulation STAR (solid lines), and EUV emission profile (dots)[10, 11].

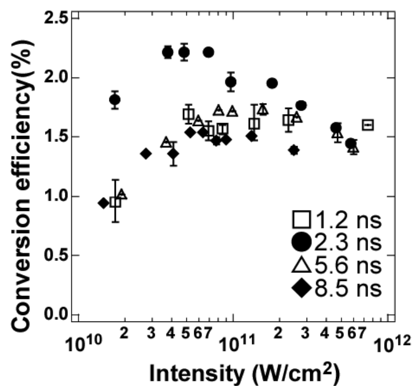

Fig 7. CE dependence on laser pulse duration[14)].

EUV CEs were also measured by changing laser pulse durations for Sn plasma. Experimental results shown in Fig. 7 indicate that the optimum pulse duration is determined by the optical depth of tin plasma for 13.5 nm light and the laser absorption rate in the EUV dominant region. The maximum CE of 2.2% is obtained with pulse duration of 2.3 ns[14)].

A simple analytical model was presented for the conversion of laser to EUV radiation[15)]. Comparison of the model prediction with experimental results (see Fig. 8) shows a good agreement under different conditions of plasma generation such as laser wavelength, intensity, and pulse duration, and target atomic numbers.

3.4 CE dependence on target density

Influence of initial density of Sn targets was quantitatively investigated[16)]. With decrease in the initial density of the target, CE from incident laser energy to output 13.5 nm light energy in a 2% bandwidth increases; the peak CE of 2.2% was attained with use of 7% low-density SnO_2 targets of 0.49 g/cm^3 irradiated with a Nd:YAG laser of 10 ns at 5x10^{10} W/cm^2. The peak CE is 1.7 times higher than that obtained with the use of solid density Sn targets.

4. Summary

Systematic studies on EUV emission from laser-produced plasma have been made. Because of high opacity, CEs are critically dependent on laser and target conditions. These results are now practically utilized for EUV source system development.

Acknowledgment

We would like to acknowledge both Gekko XII operation and EUV target fabrication groups. This work was performed under the auspices of the Leading Project by MEXT, Japan.

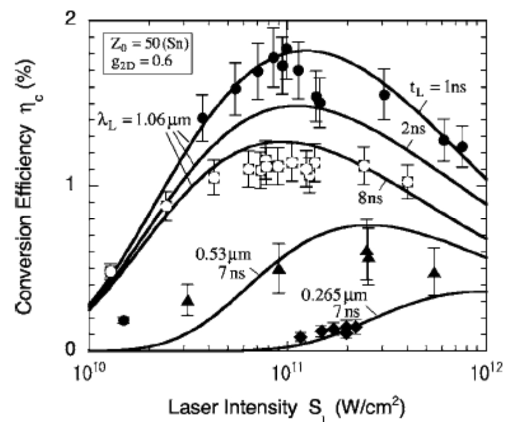

Fig.8 Comparison of CE dependences on laser wavelengths and pulse duration between the model and experiments[15)].

References

1) H. Nishimura, K. Shigemori, M. Nakai, T. Okuno, T. Hibino, R. Matsui, K. Nagai, T. Norimatsu, S. Uchida, Y. Shimada: *Proc. of Inertial Fusion Sci. and Applications* 2003, (Monterey, CA, 2004) p.1007.

2) M. Nakai, H. Nishimura, K. Shigemori, M. Nakai, T. Okuno, T. Hibino, R. Matsui, K. Nagai, T. Norimatsu, S. Uchida, Y. Shimada: *Proceeding of SPIE* 5196 (SPIE, Bellingham, WA, 2004) p.289.

3) K. Nishihara, T. Mochizuki, and H. Nishimura: The Review of Laser Engineering **32** (2004) 330 (in Japanese).

4) V. Banine: *Proc. of EUVL Source Workshop*, (Barcelona, Spain, 2006).

5) A. Sunahara, A. Sasaki, Tanuma, K Nishihara, T. Nishikawa, F. Koike, S. Fujioka, T. Aota, M. Yamaura, Y. Shimada, et al: J. Plasma and Fusion Research **11** (2007) 920.

6) K. Nishihara, T. Nishikawa, A. Sasaki, T. Kawamura, A. Sunahara, H. Furukawa, M. Murakami, H. Nishimura, Y. Shimada, M. Nakai, et al.: Proc. of Inertial Fusion Science and Applications 2003, (Monterey, CA, 2004) p.1069.

7) A. Bar-Shalom, J. Oreg, and M. Klapisch: Phys. Rev. E 56 (1997) R70.

8) Y. Shimada, H. Nishimura, M. Nakai, K. Hashimoto, M. Yamaura, Y. Tao, K. Shigemori T. Okuno, K. Nishihara, T. Kawamura, et al.: Appl. Phys. Lett. **86** (2005) 051501.

9) R. C. Spitzer, T. J. Orzechowski, D. W. Phillion, R. L. Kauffman, and C. Cerjan: J. Appl. Phys. **79** (1996) 2251.

10) Y. Tao, H. Nishimura, S. Fujioka, A. Sunahara, M. Nakai, T. Okuno, N. Ueda, K. Nishihara, N. Miyanaga, and Y. Izawa: Appl. Phys. Lett. **86** (2005) 201501.

11) Y. Tao, M. Nakai, H. Nishimura, S. Fujioka, T. Okuno, T. Fujiwara, N. Ueda, N. Miyanaga, and Y. Izawa: Rev. Sci. Instum. **75** (2004) 5173.

12) M. Yamaura, et al.: Appl. Phys. Lett. **86** (2005) 181107.

13) H. Tanaka, A. Matsumoto, K. Akinaga, A. Takahashi, and T. Okada: Appl. Phys. Lett. **87** (2005) 041503.

14) T. Ando, S. Fujioka, H. Nishimura, N. Ueda, Y. Yasuda, K. Nagai, T. Norimatsu, M. Murakami, K. Nishihara, N. Miyanaga, Y. Izawa et al.: Appl. Phys. Lett. **89** (2006) 151501.

15) M. Murakami, S. Fujioka, H. Nishimura, T. Ando, N. Ueda, Y. Shimada, and M. Yamaura: Phys. Plasmas **13** (2006) 033107.

16) T. Okuno, S. Fujioka, H. Nishimura, Y. Tao, K. Nagai, Q. Gu, N. Ueda, T. Ando, K. Nishihara, T. Norimats, et al.: Appl. Phys. Lett. **88** (2006) 161501.